Ferroelectric Behavior in Metal-Containing Liquid Crystals: A Structure-Activity Study

M. J. Baena,† J. Barberá,‡ P. Espinet,*,† A. Ezcurra,§ M. B. Ros,‡ and J. L. Serrano*,‡

Contribution from Departamento de Química Inorgánica, Facultad de Ciencias, Universidad de Valladolid, 47005 Valladolid, Spain, Química Orgánica, Facultad de Ciencias-I.C.M.A., Universidad de Zaragoza-C.S.I.C., 50009 Zaragoza, Spain, and Departamento de Física Aplicada II, Facultad de Ciencias, Universidad del Pais Vasco, Aptdo. 644, 48080 Bilbao, Spain

Received July 30, 1993®

Abstract: The synthesis and physical characterization (thermotropic and ferroelectric behavior) of eight *ortho*-palladated dimers $[Pd_2(\mu\text{-}Cl)_2L^*_2]$ is reported. They are derived from chiral imines HL* (HL* = *p*-$R^1OC_6H_4CH{=}NC_6H_4$-OR^2-*p*, with R^1, R^2, or both equal to (*R*)- or (*S*)-1-methylheptyl). The chiral imines, which contain one or two stereogenic centers, are not liquid crystals themselves. However, the dimeric complexes, which contain two or four stereogenic centers in their structure, exhibit both SmA and SmC* mesophases and enable the first comparative structure–activity study on metal-containing ferroelectric liquid crystals to be made. The ferroelectric properties obtained are better when there are chiral chains on the *ortho*-metalated aromatic rings, because the fixed conformation of these rings diminishes the chiral tail freedom, thus allowing a better coupling of molecular dipoles. The complexes with two chiral tails show important Ps_{max} values in the range 44–131 nC·cm^{-2}. The complex with four chiral chains ($R^1 = R^2 =$ (*R*)-methylheptyl) is the first such compound ever reported containing four stereogenic centers; furthermore, it shows a remarkably high Ps_{max} value of 206 nC·cm^{-2}, the highest value reported so far for a metal-containing liquid crystal.

Introduction

The existence and consequences of polar order in condensed matter are of great importance from both a scientific and a technological point of view. Ferroelectric liquid crystals (FLC) are the only fluid phases possessing such order, which makes them of special interest.[1]

Since the discovery of the first FLC, considerable efforts have been made to synthesize compounds exhibiting the ferroelectric chiral smectic C phase (SmC*), and the versatility of organic chemistry has produced a bewildering variety of chemical structures displaying this behavior. Many ferroelectric organic liquid crystals of low molecular weight bearing stereogenic centers either in the flexible hydrocarbon terminal chains,[1] in the rigid core,[2,3] or in the flexible spacer in dimeric structures,[4,5] as well as related side-chain polymeric compounds,[1c,6,7] have been reported.

During the last decade, a new class of mesogen incorporating transition metals has burst into the liquid crystal field, giving rise to a great variety of mesophases.[8] By introducing chirality into these structures, chiral nematic (cholesteric), smectic, or discotic phases should also be obtained. In the case of the smectic C phase, this implies the production of promising ferroelectric fluid materials where the presence of metal atoms might render special electrical, optical, and/or magnetic properties.

The first steps in developing this exciting idea have already been made with encouraging results. In 1989 we reported the first organo transition metal compound displaying ferroelectric behavior;[9] it was an *ortho*-palladated dimer derived from an azine with a chiral carboxylato intermetallic bridge (Figure 1, **I**), and the material consisted of a mixture of *cis* and *trans* isomers which showed the characteristic FLC switching behavior when an ac field was applied. More recently the first examples of paramagnetic complexes exhibiting FLC properties were described;[10] in this case, two chiral salicilaldiminates of copper(II) and vanadium(IV) were studied for which spontaneous polarization maxima around 20 nC·cm^{-2} were found (Figure 1, **II**). As a third example of ferroelectric metallomesogens, we have also reported monomeric β-diketonate palladium complexes derived from *ortho*-palladated imines which show similar polarization values (Figure 1, **III**).[11] All these complexes are singular but clear examples proving that ferroelectricity can be obtained in metallomesogens and opening up the unexplored field of the molecular structure/ferroelectric activity relationship in metal-containing liquid crystals.

The present paper aims to be a pioneer in this area of study and reports the first comparative series of metal-containing liquid crystals for which the ferroelectric behavior has been fully characterized.

Our previous work on *ortho*-palladated compounds had shown that dinuclear Pd(II) complexes derived from Schiff bases have a rich mesomorphism when a halogen intermetallic bridge is present. Furthermore, broad ranges of smectic C phase occur

† Universidad de Valladolid.
‡ Universidad de Zaragoza-C.S.I.C.
§ Universidad del Pais Vasco.
• Abstract published in *Advance ACS Abstracts,* February 1, 1994.

(1) For an introduction to FLC, see: (a) Lagerwall, S. T.; Otterholm, B.; Skarp, K. *Mol. Cryst. Liq. Cryst.* **1987**, *152*, 503. (b) Beresnev, L. A.; Blinov, L. M.; Osipov, M. A.; Pikin, S. A. *Mol. Cryst. Liq. Cryst.* **1988**, *158A*, 3. (c) Walba, D. M. Ferroelectric Liquid Crystals. A Unique State of Matter. In *Advances in the Synthesis and Reactivity of Solids*; Mallouk, T. E., Ed.; JAI Press Ltd.: Greenwich, CT, 1991; Vol. 1, p 173.

(2) Nakauchi, J.; Uematsu, M.; Sakashita, K.; Kageyama, Y.; Hayashi, S.; Ikemoto, T.; Mori, K. *Jpn. J. Appl. Phys.* **1989**, *28*, L1258.

(3) Stegemeyer, H.; Meister, R.; Ellermann, K. H.; Altenbach, H. J.; Sucrow, W. *Liq. Cryst.* **1992**, *11*, 667.

(4) Ujiie, S.; Iimura, K. *Chem. Lett.* **1990**, 1031.

(5) Marcos, M.; Omenat, A.; Serrano, J. L.; Sierra, T.; Ezcurra, A. *Adv. Mater.* **1992**, *4*, 285.

(6) Dumon, M.; Nguyen, H. T.; Mauzac, M.; Destrade, D.; Achard, M. F.; Gasparoux, H. *Macromolecules* **1990**, *23*, 355.

(7) *Polym. Adv. Tech.* (special topic issue: Ferroelectric Liquid Crystal Polymers); Lewin, M., Jaffe, M., Wendorff, J. H., Tsuchida, E., Kremer, F., Eds.; John Wiley & Sons: New York, 1992, Vol. 3, No. 5.

(8) For reviews, see: Giroud-Godquin, A. M.; Maitlis, P. M. *Angew. Chem.* **1991**, *103*, 370. *Angew. Chem., Int. Ed. Engl.* **1991**, *30*, 375. Espinet, P.; Esteruelas, M. A.; Oro, L. A.; Serrano, J. L.; Sola, E. *Coord. Chem. Rev.* **1992**, *117*, 215.

(9) Espinet, P.; Etxebarría, J.; Marcos, M.; Pérez, J.; Remón, A.; Serrano, J. L. *Angew. Chem.* **1989**, *101*, 1076. *Angew. Chem., Int. Ed. Engl.* **1989**, *28*, 1065.

(10) Marcos, M.; Serrano, J. L.; Sierra, T.; Giménez, M. J. *Angew. Chem.* **1992**, *104*, 1523; *Angew. Chem., Int. Ed. Engl.* **1992**, *31*, 1471.

(11) Baena, M. J.; Espinet, P.; Ros, M. B.; Serrano, J. L.; Ezcurra, A. *Angew. Chem.* **1993**, *32*, 1203; *Angew. Chem., Int. Ed. Engl.* **1993**, *105*, 1260.

0002-7863/94/1516-1899$04.50/0 © 1994 American Chemical Society

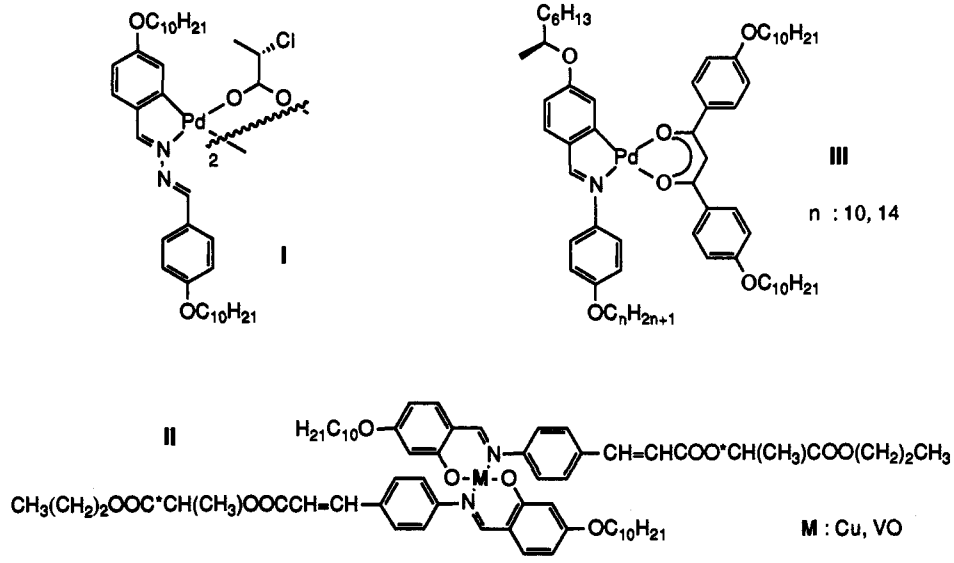

Figure 1. Ferroelectric metal-containing liquid crystal reported in the literature.

Chart 1

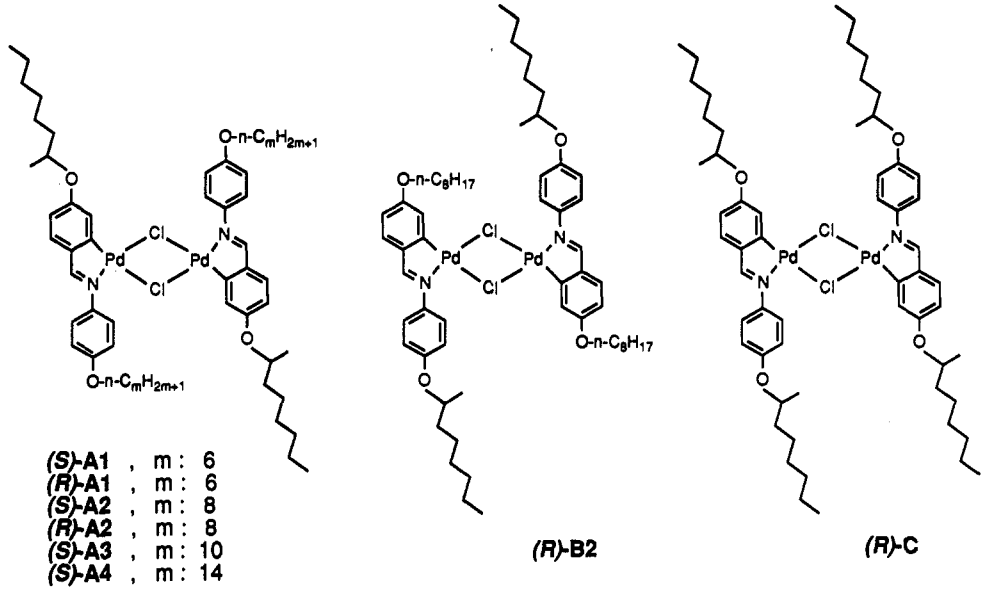

when the halogen is chlorine.[12-14] Bearing this in mind, we undertook the introduction of chirality in the most suitable structures and describe here eight new *ortho*-palladated dimers derived from chiral alkylidenamines: (*S*,*S*)-**A1**; (*R*,*R*)-**A1**; (*S*,*S*)-**A2**; (*R*,*R*)-**A2**; (*S*,*S*)-**A3**; (*S*,*S*)-**A4**; (*R*,*R*)-**B2**; and (*R*,*R*,*R*,*R*)-**C** (Chart 1), which allow several comparisons to be made within the series. The discussion focuses on the influence on the ferroelectric behavior of (i) the length of the achiral terminal chain; (ii) the position of the chiral tails; and (iii) the number of chiral tails per molecule.

Due to the complexes studied having two or four stereogenic centers with the same configuration, for the sake of simplification, we will commonly name them by a unique (*S*)- or (*R*)-.

Results

Synthesis. The synthesis of the compounds starting from commercial *p*-hydroxybenzaldehyde (**1**), *p*-acetamidophenol (**2**), and *p*-nitrophenol (**3**) is outlined in Scheme 1.

The achiral alkoxybenzaldehydes **4** and alkoxyacetamides were obtained by a Williamson etherification with the corresponding alkylbromide, followed by an amino deprotection reaction in the case of the anilines **6**.[15] As an alternative route, the chiral alkoxyaniline was synthesized starting from *p*-nitrophenol (**3**) followed by the reduction of the nitro group by $SnCl_2 \cdot H_2O$ according to the method described by Bellamy.[16]

The chiral tail used in the compounds reported here was in each case the 1-methylheptyloxy group prepared from the commercial (*R*)-(−)- or (*S*)-(+)-2-octanol available from Aldrich and used as received; the results obtained on the products revealed that, in spite of the catalog specifications, their enantiomeric purities are different (to be discussed later). The (1-methylheptyloxy)phenyl derivatives were synthesized by means of a nucleophilic substitution, via a Mitsunobu reaction[17] (method II) that takes place with total inversion of the asymmetric center configuration.[17]

The condensation of the corresponding intermediates **4** and **6** afforded the chiral imines **7**. On heating **7** with $Pd_3(OAc)_6$ in acetic acid, the imines were *ortho*-palladated to give the acetato-

(12) Barberá, J.; Espinet, P.; Lalinde, E.; Marcos, M.; Serrano, J. L. *Liq. Cryst.* **1987**, *2*, 833.
(13) Marcos, M.; Ros, M. B.; Serrano, J. L. *Liq. Cryst.* **1988**, *8*, 1129.
(14) Ros, M. B.; Ruiz, N.; Serrano, J. L.; Espinet, P. *Liq. Cryst.* **1991**, *9*, 77.
(15) Keller, P.; Liébert, L. *Solid State Phys., Suppl. 14*, **1978**, 19.
(16) Bellamy, F. D.; Ou, K. *Tetrahedron Lett.* **1984**, *25*, 839.
(17) Mitsunobu, O. *Synthesis* **1981**, 1.

Scheme 1

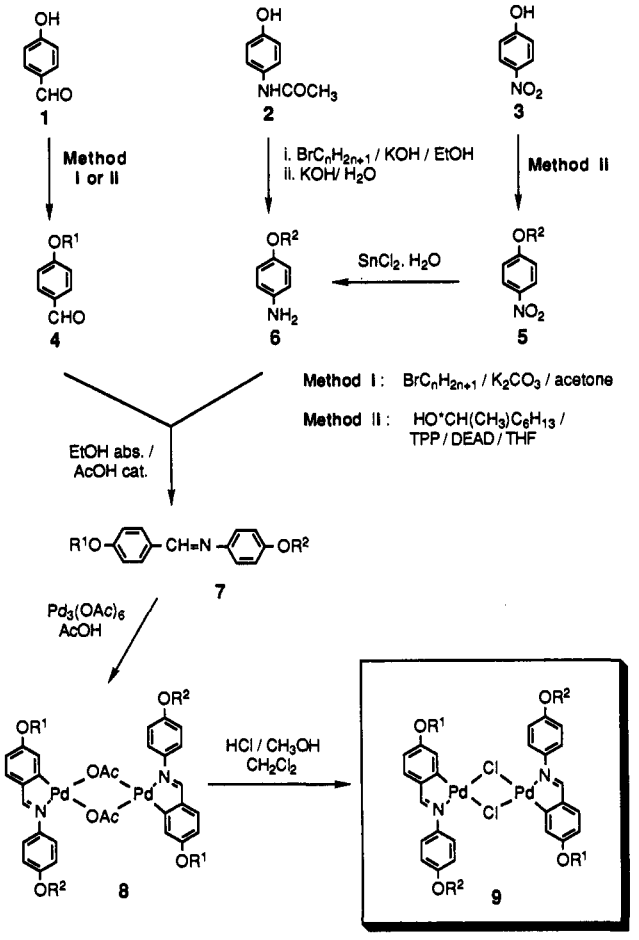

bridged complexes **8**, which were used in the last step of the synthesis. (The high solubility of the corresponding complex with four chiral chains made it easier to obtain the pure chloro-bridged complex first. The acetato-bridged complex was then prepared, for identification purposes only, starting from the pure chloro-bridged complex; see Experimental Section.)

The dimeric nature of **8** can give rise to *cis* and *trans* isomers; in addition, since the open-book structure does not undergo inversion, the *trans* isomer is a chiral structure (we will use Λ and Δ to label its two enantiomers) that will give rise to diastereoisomers when the ligands are chiral.[9,18,19] The ^{1}H-NMR spectra of the complexes **8** show that they are indeed mixtures of 6–9% of the *cis* isomer and 94–91% of the two *trans* diastereoisomers (Δ-(*R*) and Λ-(*R*) or Δ-(*S*) and Λ-(*S*), depending on the chirality of the imine) in different proportions.[18] For the acetato-bridged complexes with chiral chains on the *ortho*-palladated rings (corresponding to the chloro-bridged compounds **A** or **C**) the two *trans* diastereoisomers are in the ratio 64–69/36–31, while in the compound with chiral chains on the free rings only (precursor of complex **B2**) they are in a *ca.* 50/50 proportion.

Treatment of **8** in methanol/dichloromethane with HCl gives the planar chiral chloro-bridged palladium complexes **9**. Their ^{1}H-NMR spectra show that only the *trans* isomers of these complexes are formed.[19]

Liquid Crystal Behavior of the Chloro-Bridged Complexes. The thermal data of the chloro-bridged palladium complexes **9** are summarized in Table 1 and Figure 2.

In general, as is usual in this type of chloro *ortho*-palladated mesogens,[12–14] the compounds show high liquid-crystal-phase stabilities with smectic-phase ranges about 100 degrees. All the compounds show the potentially ferroelectric SmC* phase enantiotropically, with the exception of complex **C**, which exhibits only a monotropic SmC* phase, as shown in Figure 2. Above the SmC* phase a broad range SmA phase is also observed. Differential scanning calorimetry measurements indicate that the SmA–SmC* transitions are accompanied by very small enthalpy changes (0.2–0.4 kJ·mol^{-1}).

Table 1. Transition Temperatures for the Chloro-Bridged Complexes **9**

compd	transition[a]	temp (°C)	Δ*H* (kJ·mol^{-1})
(*S*)-**A1**	K_1–K_2	110.4	16.26
	K_2–SmC*	131.5	22.50
	SmC*–SmA	139.9	0.13[b]
	SmA–I	231.0	7.64
(*R*)-**A1**	K_1–K_2	109.7	16.58
	K_2–SmC*	131.4	23.09
	SmC*–SmA	136.1	0.21[b]
	SmA–I	229.2	6.31
(*S*)-**A2**	K_1–K_2	114.7	18.48
	K_2–SmC*	127.7	12.75
	SmC*–SmA	157.3	0.14
	SmA–I	223.6	7.93
(*R*)-**A2**	K_1–K_2	115.2	15.94
	K_2–SmC*	127.9	13.05
	SmC*–SmA	155.8	0.40
	SmA–I	219.9	7.80
(*S*)-**A3**	K–SmC*	108.4	16.37
	SmC*–SmA	149.3	0.56
	SmA–I	218.7	8.00
(*S*)-**A4**	K–SmC*	101.4	16.33
	SmC*–SmA	123.8	0.33
	SmA–I	209.1	8.16
(*R*)-**B2**	K–SmC*	132.3	13.04
	SmC*–SmA	175.7	0.23
	SmA–I	230.1	8.08
(*R*)-**C**	K–SmA	113.7	35.45
	SmA–I	121.0	3.97
	SmA–SmC*[c]	88.3	–0.30

[a] K, crystal; SmA, smectic A phase; SmC*, chiral smectic C phase; I, isotropic liquid. [b] Data from the cooling process. [c] Monotropic transition.

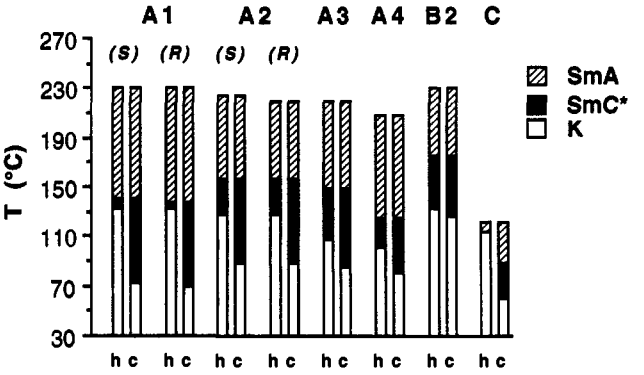

Figure 2. Mesophase ranges of the chloro-bridged complexes **9** in the heating (h) and cooling (c) processes.

Mesophase Characterization of the Chloro-Bridged Complexes. The mesophases were first identified according to their textures[20] observed by optical microscopy. In the heating process the SmC* phase appears on melting as a blurred-*schlieren* texture which gives rise to mielinic textures in the SmA phase. On cooling the isotropic liquid, the SmA phase appears, *via batônnets*, as a focal-conic texture. At the SmA–SmC* transition temperature a clear broken focal-conic texture was observed on cooling the SmA phase. For some of these complexes helix unwinding lines were detected at the SmC* phase (Figure 3). In all the complexes the SmC* texture, with very slight changes, remains on crystallization.

The mesophases of all complexes **9** were also characterized by X-ray diffraction at several temperatures. The SmA and SmC*

(18) Espinet, P.; Lalinde, E.; Marcos, M.; Pérez, J.; Serrano, J. L. *Organometallics* **1990**, *9*, 555.
(19) Ciriano, M. A.; Espinet, P.; Lalinde, E.; Ros, M. B.; Serrano, J. L. *J. Mol. Struct.* **1989**, *196*, 327.
(20) Gray, G. W.; Goodby, J. W. G. *Smectic Crystal Textures and Structures*; Leonard Hill: Glasgow, 1984.

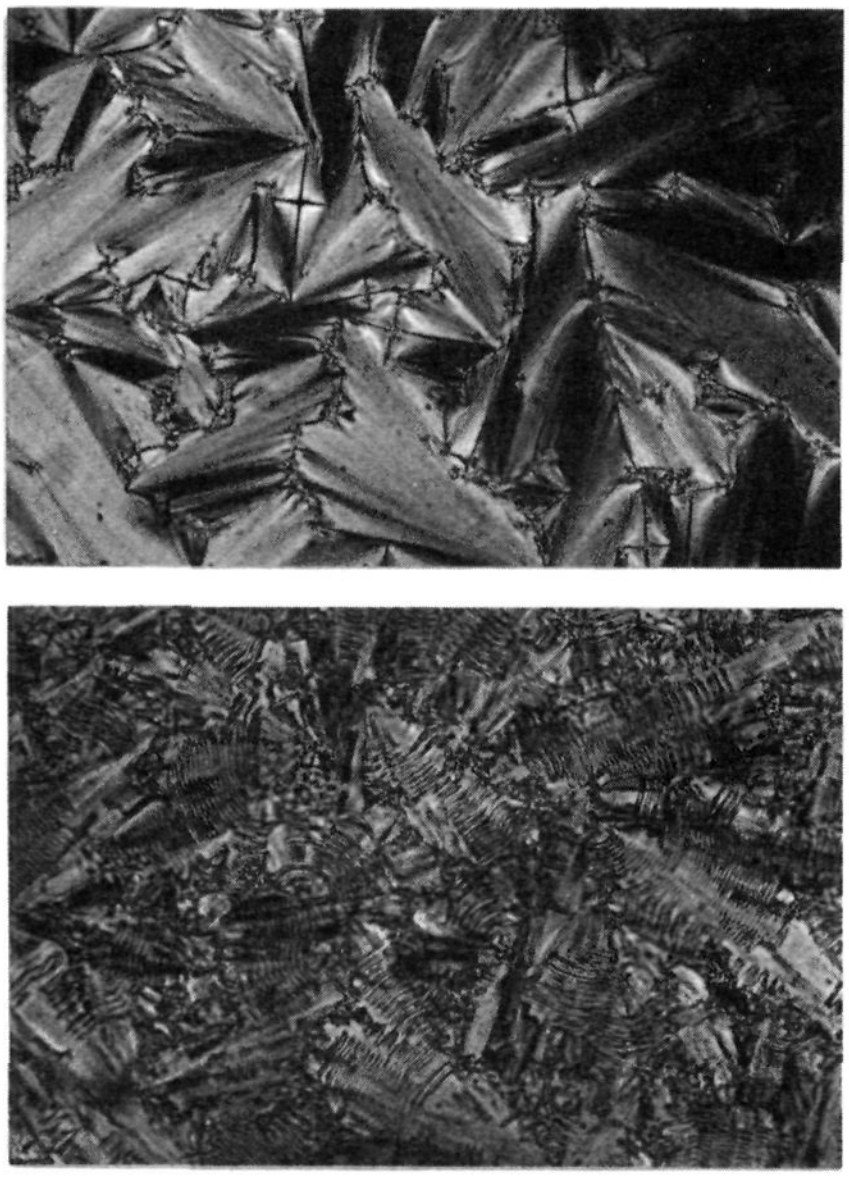

Figure 3. Photomicrograph of complex (*S*)-**A2** in the SmA phase at 178 °C (top) and in the SmC* phase at 135 °C (bottom) viewed between crossed polarizers.

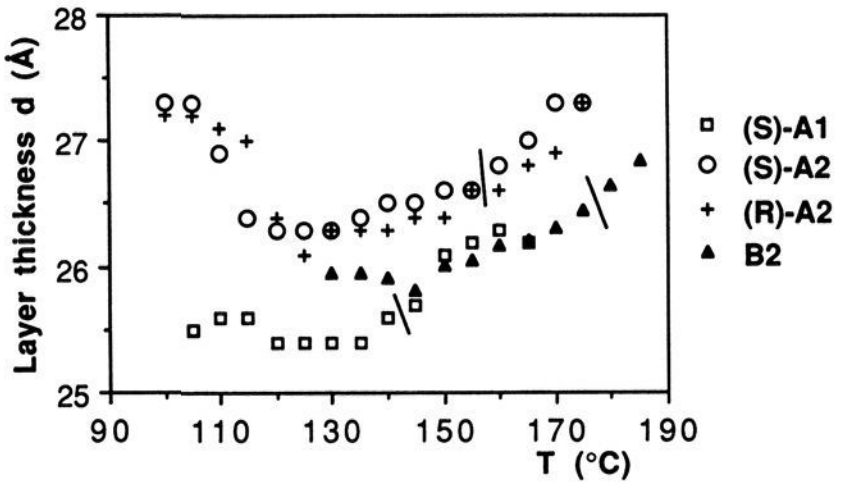

Figure 4. Temperature dependence of the layer thickness of some chloro-bridged complexes **9** at the mesophase state on the cooling process. (The sign (/) indicates the SmC*–SmA transition.)

nature of the phases was confirmed by the presence of a sharp peak at low angles and the absence of any other Bragg peak. From the scattering angle of this reflection, the Bragg equation gives the layer spacing. No great differences in layer thickness were observed between the SmA and SmC* phases, indicating very small tilt angles for the SmC* phase. For some of the chloro-bridged compounds a gradual decrease of the layer periodicity was observed, as expected, on lowering the temperature in the SmC* phase. For others, more significantly for **A1** and **A2**, an increase in the layer spacing occurs through this phase (Figure 4). This could be due to a loss of conformational freedom at lower temperatures, which in turn causes the more extended chains to overcome the effect of tilting.

A comparison of the layer thickness for the complexes in their SmA phase and the length of the ligands in a fully extended conformation (estimated from Dreiding stereomodels) shows the measured lengths to be 6–7 Å shorter than the estimated layer spacing, suggesting that the terminal chains are rather disordered. These differences are similar to those found in other mesogenic palladium complexes[21] and small enough to rule out any significant interdigitation of molecules in the mesophase.[22]

Ferroelectric Properties of the Chloro-Bridged Complexes. The following properties were evaluated for the eight complexes: spontaneous polarization (Ps); response time (τ); viscosity (γ_c); and spontaneous polarization corrected with regard to the tilt angle (Po). Response times and rotational viscosities were calculated from the Ps value applying the equation $\tau = 1.75\gamma_c/PsV$. Due to the rather high viscosity of these materials and in order to prevent their thermal decomposition in prolonged heatings, the measurements were performed using cells made of two golden-brass electrodes and filling was achieved in the SmA phase. The data are collected in Table 2.

Figures 5 and 6 show the dependence of the Ps and τ versus temperature. While Figure 5a compares the variation of the polarization for different terminal chain lengths, Figure 5b illustrates the influence of both the position of the chiral chain and the number of chains. The increase in Ps values of all the compounds is gradual when the temperature decreases. Parts a and b of Figure 6 show similar comparative studies for the response times.

Discussion

A new class of ferroelectric liquid crystal based on molecules containing metal atoms and bearing two or four chiral chains in their structure has been studied; even in organic FLCs very few examples of compounds containing more than one chiral tail have been reported.[23]

It is worth noting that none of the Schiff bases used as ligands are themselves liquid crystals. This means, once again, that complexation is a useful way to generate mesogenic behavior.[8] The dimeric structure of the complexes fixes the disposition of the imine molecules and leads to a better arrangement of the organic ligand that contributes to the appearance of liquid crystal order. This contribution is reinforced by the increased intermolecular interactions induced by the metal atom.

From the viewpoint of the molecular structure/mesogenic properties relationship, several aspects are of note. Firstly, when the chiral chains are in the *ortho*-palladated rings, terminal chains in the other ring with 8 or 10 carbon atoms (compounds **A2** and **A3**) give rise to the broadest enantiotropic SmC* phases (the small differences between the (*S*) and (*R*) enantiomers are due to their different purities, as discussed below). Secondly, the change in the position of the chiral chain (compound **B2**) gives rise to a more stable SmC* phase. This can be attributed to lower steric hindrance of the chiral chain when it is in the anilinic ring, due to its higher mobility and spacing out from the crowded, rigid core. This allows more efficient intramolecular packing of the chains, favoring the molecular interactions that stabilize the SmC* phase.

With regard to complex **C**, remarkable changes occur when the molecule has four chiral chains. Although both smectic A and C* phases appear, a dramatic decrease in the mesophase stability is produced, possibly because the severe steric hindrance disturbs the otherwise efficient inter- and intramolecular packing of the chains. A positive effect[24] is that the melting point is somewhat reduced and a SmC* phase below 90 °C is obtained.

(21) Espinet, P.; Pérez, J.; Marcos, M.; Ros, B.; Serrano, J. L.; Barberá, J.; Levelut, A. M. *Organometallics* **1990**, *9*, 2028.
(22) Barberá, J.; Levelut, A. M.; Marcos, M.; Romero, P.; Serrano, J. L. *Liq. Cryst.* **1991**, *10*, 119.
(23) (a) Bomelburg, J.; Hansel, Ch.; Heppke, G.; Hollidt, J.; Lotzsch, D.; Scherf, K. D.; Wuthe, K.; Zaschke, H. *Mol. Cryst. Liq. Cryst.* **1990**, *192*, 355 and references therein. (b) Kobayashi, S.; Ishibashi, S. *Mol. Cryst. Liq. Cryst.* **1992**, *220*, 1 and references therein. (c) Scherowsky, G. *Polym. Adv. Tech.* **1992**, *3*, 219.
(24) Baena, M. J.; Espinet, P.; Ros, M. B.; Serrano, J. L. *Angew. Chem.* **1991**, *103*, 716; *Angew. Chem., Int Ed. Engl.* **1991**, *30*, 711.

Table 2. Ferroelectric Properties of the Chloro-Bridged Complexes and of the Mixtures Based on the Ligands

chloro-bridged complexes								ligands		
compd	conf	Ps max (nC·cm^{-2})	Ps[a] (nC·cm^{-2})	τE[a] (μsV·μm^{-1})	γ_c[a] (Pa·s)	θ[a,b] (deg)	Po[a,c] (nC·cm^{-2})	compd[e]	%[f] (mol)	Ps ext[g,h] (nC·cm^{-2})
A1	S	−58	−58	1126	0.37	13.8	243	**LA1**	14.7	−30
A1	R	+48	+45	1027	0.26	13.8	189	**LA1**	14.9	+32
A2	S	−131	−96	1479	0.81	14.7	378	**LA2**	15.0	−36
A2	R	+105	+81	1916	0.88	15.5	303	**LA2**	14.9	+36
A3	S	−69	−56	553	0.16	15.0	216	**LA3**	16.8	−37
A4	S	−44	−43	3800	0.93	12.7	196	**LA4**	14.8	−24
B2	R	+47	+40	744	0.17	13.8	168	**LB2**	15.2	+21
C	R	+206	+183	39 956	41.80	*d*		**LC**	*i*	

[a] Data measured at $T_c - T = 20$ °C (Tc, SmA–SmC* transition temperature determined by DSC). [b] Determined by comparing the layer thickness in the SmA and SmC* phases from X-ray data. [c] Po = Ps/sin θ. [d] Crystallization prevented the evaluation of this magnitude at Tc − T = 20 °C. [e] Notation: LX, organic ligand base of complex X. [f] Percentage of the corresponding organic ligand in the binary mixture with the SmC achiral host: 4-(hexyloxy)phenyl 4′-(decyloxy)benzoate (K 62.5 °C SmC 78.2 °C SmA 84.5 °C N 90.5 °C I). [g] Optical tilt angles of 22–25° have been determined for these mixtures at 20 °C below the SmA–SmC* transition. [h] From data measured at 20 °C below the SmA–SmC* transition and considering a linear relationship with the concentration. [i] This mixture was not evaluated because this ligand could not be isolated with enough purity to be used in this study.

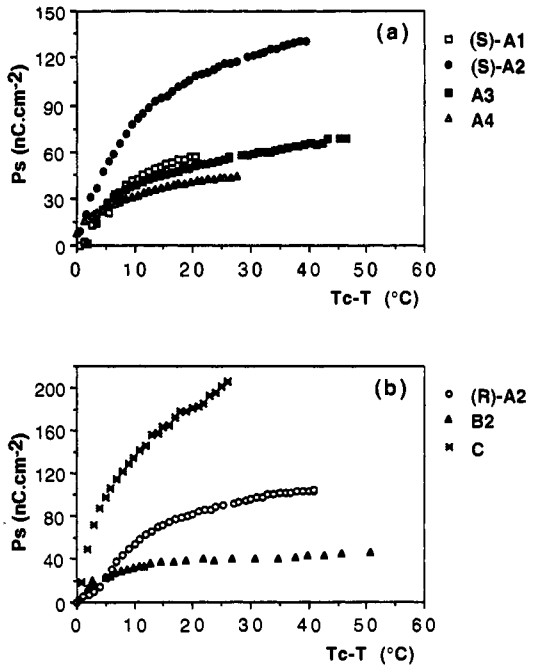

Figure 5. Temperature dependence of the polarization of the chloro-bridged complexes **9**: (a) influence of the achiral tail length, (b) influence of the chiral tail position and the number of chiral tails.

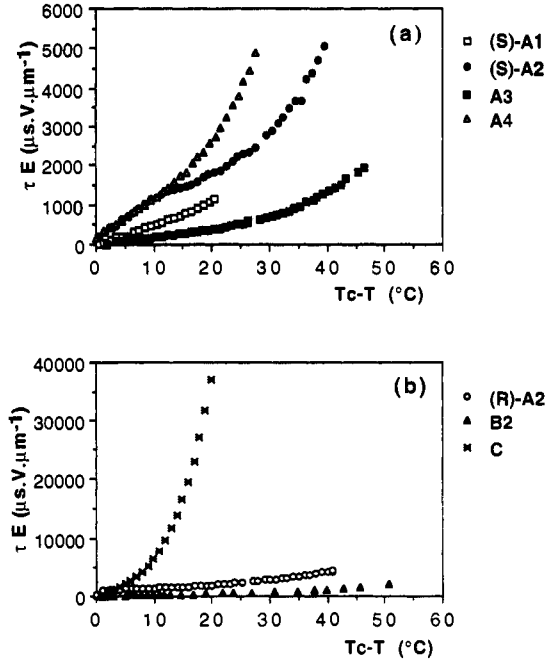

Figure 6. Temperature dependence of the response times of the chloro-bridged complexes **9**: (a) influence of the achiral tail length, (b) influence of the chiral tail position and the number of chiral tails.

As far as the structure/ferroelectric activity relationship is concerned, the trends established are similar to those observed in organic FLCs.

Carbon chain length proves to play an important role not only in the thermal stability of the SmC* phase but also in the magnitude of the Ps in this phase,[25] which reach maximum values in the octyloxy derivative **A2** (see Table 2 and Figure 5a). On the basis of these results we selected the octyloxy-chain length for complexes of type **B**.

Unexpected differences in the ferroelectric magnitudes for both pairs of enantiomers (*S*)-**A1**/(*R*)-**A1** and (*S*)-**A2**/(*R*)-**A2** were observed (see Table 2). Since the spontaneous polarization in liquid crystals is a property derived from the chirality of the SmC* phase, its magnitude is dependent on the optical purity of the sample.[26] With regard to this matter we investigated the rotatory power of the complexes, the chiral imines used as ligands, and the commercial alcohols (Aldrich) used in their synthesis; the results are collected in Table 3.

Table 3. Rotatory Power of the Starting Alcohols and Some of the Ligands and Chloro-Bridged Complexes Studied

compd	$[\alpha]_D^{20}$	*c* (g/100 mL)	solvent
(*R*)-2-octanol	−9.3	ρ: 0.838 g·cm^{-3}	neat
(*S*)-2-octanol	+8.7	ρ: 0.822 g·cm^{-3}	neat
(*R*)-**A1**	+19.7	1.24	$CHCl_3$
(*S*)-**A1**	−20.6	1.22	$CHCl_3$
(*R*)-**A2**	+19.4	1.79	$CHCl_3$
(*S*)-**A2**	−20.2	1.84	$CHCl_3$
(*R*)-**LA1**[a]	+15.2	4.17	toluene
(*S*)-**LA1**	−15.9	4.13	toluene
(*R*)-**LA2**	+3.50	2.05	$CHCl_3$
	+16.0	4.21	toluene
(*S*)-**LA2**	−3.52	2.03	$CHCl_3$
	−17.2	4.18	toluene

[a] Notation: LX, organic ligand of complex X.

In the case of the complexes and ligands, lower rotatory powers of the (*R*) enantiomers were measured, with differences of around 5–7%. For the rotatory powers of the commercial (*R*)- and (*S*)-2-octanols used as starting materials, similar differences were also detected with neat samples and using the density values from

(25) (a) Inukai, T.; Saitoh, S.; Inoue, H.; Miyazawa, K.; Terashima, K.; Fukurawa, K. *Mol. Cryst. Liq. Cryst.* **1986**, *141*, 251. (b) Nakauchi, J.; Kageyawama, Y.; Hayashi, S.; Sakashita, K. *Bull. Chem. Soc. Jpn.* **1989**, *62*, 1685.

(26) (a) Dubal, H.-R.; Escher, C.; Ohlendorf, D. *Ferroelectrics* **1988**, *84*, 143. (b) Barh, CH.; Heppke, G.; Sabaschus, B. *Ferroelectrics* **1988**, *84*, 103. (c) Barh, CH.; Heppke, G.; Sabaschus, B. *Liq. Cryst.* **1991**, *9*, 31.

the Aldrich catalog; in this case the (*R*) enantiomer gave the higher value, as expected, due to the total inversion taking place during the Mitsunobu reaction. Consequently, the differences in rotatory power between enantiomers, as well as the differences observed in their transition temperatures[26b] (Table 1), can be attributed to the presence of a certain amount of the other enantiomer in the samples; this will produce a partial cancellation of ferroelectric properties such as the magnitude of the spontaneous polarization.

It is well-known that in order to obtain high Ps values, strong intermolecular coupling of the molecular dipoles should be obtained.[1] Those effects that hinder or avoid the independent mobility of the molecule or the chiral tail will contribute to this purpose.[1,3,27] This is the case in the comparison between compounds **A2** and **B2**. The *ortho*-metalation of the aldehydic ring fixes the orientation of the 1-methylheptyloxy chain[1c] more effectively in comparison with the anilinic ring, which can rotate quite freely. Hence, the mobility of the chiral tails in compound **A2** is diminished, allowing better coupling of the dipoles associated with them and giving rise to higher Ps values.

As we mentioned previously, very few examples of compounds containing more than one chiral tail are reported in the literature, but in all cases the compounds exhibit large Ps values, even larger than the sum of the Ps contribution of corresponding homologues with a single chiral chain.[23b] Similar results have been observed in the palladated derivatives reported here. Compound **C**, the first ferroelectric liquid crystal with four chiral chains ever reported, shows a remarkably high Ps value, the highest magnitude ever measured for a metallomesogen. This value is larger than the sum of the Ps values of the homologues ((*R*)-**A2** and **B2**) containing two chiral tails.

A comparison can also be made between the ligands and their corresponding complexes. The ferroelectric properties of the chiral imines were evaluated in binary mixtures with a nonchiral solvent (4-(hexyloxy)phenyl 4′-(decyloxy)benzoate; K 62.5 °C SmC 78.2 °C SmA 84.5 °C N 90.5 °C I). All of them exhibited induced SmC* phase in a range 20–30 °C, with the ferroelectric properties collected in Table 2.

Considering a linear extrapolation of the spontaneous polarization magnitudes obtained for low concentration mixtures of the chiral imines, the complexes show higher spontaneous polarization values (Ps and Po) than twice the ones of the corresponding Schiff base. These results differ from those observed for the ferroelectric copper and vanadyl complexes (Figure 1, **II**) for which a decrease of Ps was obtained on complexation.[10] This is probably due to the different structural characteristics of the copper and vanadyl complexes which can hinder the dipolar moment coupling.

The sign of Ps, both for the complexes and for the ligands, is the same as reported for other compounds bearing the 1-methylheptyloxy group as a chiral tail, i.e. negative for the (*S*) and positive for the (*R*) enantiomers.[25a,28]

Finally, all of the ferroelectric palladium complexes discussed here show a high rotational viscosity that explains the rather large response times determined for them. The response times are on the order of milliseconds and are similar to those measured for FLC polymers.[6,7] This is easily understandable taking into account the structure of these molecules with a l/d ratio rather smaller than that typically found in organic FLCs. These large molecules, in switching the electric field, must rotate describing a cone angle,[1a] which they probably do without moving their center of mass in a cooperative movement.

Experimental Section

Synthesis. The achiral *p*-(octyloxy)benzaldehyde and *p*-alkoxyanilines were synthesized following methods described elsewhere.[15] All compounds gave satisfactory C, H, and N analyses and ^{1}H-NMR and IR spectra. Since the ^{1}H-NMR and IR data are very similar for the series, full details are given only for representative types of intermediate compounds and for all the complexes **8** and **9**.

Procedure for Introducing the (*R*)- or (*S*)-1-Methylheptyloxy Group (Method II). To a nitrogen-flushed flask containing 8 mmol of 4-hydroxybenzaldehyde or 4-nitrophenol and 1.25 equiv of triphenylphosphine (TPP) dissolved in 150 mL of dry THF was added via syringe a solution of 8.08 mmol of the corresponding isomer of 2-octanol in 20 mL of dry THF. Then, 1.25 equiv of diethyl azodicarboxylate (DEAD) dissolved in 40 mL of dry THF was added dropwise in 30 min. The reaction mixture was stirred for 19–22 h. Water (5 drops) was added, and the stirring was continued for 1 h. The reaction mixture was evaporated to dryness, and the crude residue was treated with a hexane/ethyl acetate (70/30) mixture and filtered through a short pad of silica gel. The filtrate was evaporated, and the resulting ether derivative was purified by flash chromatography on silica gel.

Analytical Data for the (*R*)- or (*S*)-((1-Methylheptyl)oxy)phenyl Derivatives. (*R*)-*p*-((1-methylheptyl)oxy)nitrobenzene: liquid, ^{1}H-NMR (80 MHz, $CDCl_3$) δ 0.88 (t, 3H), 1.20–1.50 (m, 8H), 1.34 (d, J = 6.1 Hz, 3H), 1.50–2.00 (m, 2H), 4.45 (m, 1H), 6.91 (d, J = 9.4 Hz, 2H), 8.18 (d, J = 9.4 Hz, 2H). IR (NaCl) cm^{-1}: 1516, 1497 (ν NO_2 as), 1344 (ν NO_2 s), 1265 (ν COC). Yield: 84%.

(*S*)- and (*R*)-*p*-((1-Methylheptyl)oxy)benzaldehyde: liquids, ^{1}H-NMR (300 MHz, $CDCl_3$) δ 0.85 (t, 3H), 1.20-1.43 (m, 8H), 1.30 (d, J = 6.1 Hz, 3H), 1.55 (m, 1H), 1.75 (m, 1H), 4.45 (m, 1H), 6.94 (d, J = 8.9 Hz, 2H), 7.70 (d, J = 8.9 Hz, 2H), 9.84 (s, 1H). IR (NaCl) cm^{-1}: 1701 (ν C=O), 1259 (ν COC). Yield: 65–70%.

Synthesis of (*R*)-*p*-((1-Methylheptyl)oxy)aniline. A mixture of 10 mmol of (*R*)-*p*-((1-methylheptyl)oxy)nitrobenzene and 50 mmol of $SnCl_2 \cdot 2H_2O$ in 20 mL of absolute ethanol was refluxed under nitrogen for 30 min. After cooling, the reaction mixture was poured into ice/water. The solution pH was turned slightly basic (7–8) by addition of solid K_2CO_3. The aniline was extracted with ether, washed with a saturated solution of NaCl, and dried with anhydrous $MgSO_4$. The solvent was distilled off, and the aniline was used without further purification: liquid, ^{1}H-NMR (300 MHz, $CDCl_3$) δ 0.88 (t, J = 7 Hz, 3H), 1.20–1.63 (m, 9H), 1.23 (d, J = 6.1 Hz, 3H), 1.68 (m, 1H), 3.4 (br s, 2H), 4.16 (m, 1H), 6.63 (d, J = 8.9 Hz, 2H), 7.30 (d, J = 8.9 Hz, 2H). IR (NaCl) cm^{-1}: 3433, 3360 (ν NH_2), 1628 (δ NH_2), 1235 (ν COC). Yield: 89%.

Procedure to Obtain the Schiff Bases 7. The Schiff bases were synthesized by acetic acid-catalyzed condensation of the corresponding substituted aldehyde and the respective substituted aniline in ethanol, as described elsewhere.[15] Yields: 60–90%.

Analytical Data for Compounds 7. (*S*)-4-((1-Methylheptyl)oxy)-benzylidene-4′-(hexyloxy)aniline: mp 60.2 °C.

(*R*)-4-((1-Methylheptyl)oxy)benzylidene-4′-(hexyloxy)aniline: mp 61.2 °C.

(*S*)-4-((1-Methylheptyl)oxy)benzylidene-4′-(octyloxy)aniline: mp 57.4 °C. ^{1}H-NMR (300 MHz, $CDCl_3$): δ 0.80–0.90 (m, 6H), 1.20–1.50 (m, 20H), 1.30 (d, J = 5.9 Hz, 3H), 1.60 (m, 1H), 1.65–1.85 (m, 3H), 3.95 (t, J = 6.6 Hz, 2H), 4.42 (m, 1H), 6.88 (d, J = 9.0 Hz, 2H), 6.92 (d, J = 8.8 Hz, 2H), 7.17 (d, J = 9.0 Hz, 2H), 7.78 (d, J = 8.8 Hz, 2H), 8.37 (s, 1H). IR (Nujol) cm^{-1}: 1628 (ν C=N), 1250 (ν COC). Anal. Calcd for $C_{29}H_{43}NO_2$: C 79.59%, H 9.90%, N 3.20%. Found: C 80.00%, H 9.96%, N 3.25%.

(*R*)-4-((1-Methylheptyl)oxy)benzylidene-4′-(octyloxy)aniline: mp 58.5 °C. ^{1}H-NMR (300 MHz, $CDCl_3$): identical to the former. Anal. Calcd for $C_{29}H_{43}NO_2$: C 79.59%, H 9.90%, N 3.20%. Found: C 79.92%, H 9.95%, N 3.16%.

(*S*)-4-((1-Methylheptyl)oxy)benzylidene-4′-(decyloxy)aniline: mp 60.3 °C.

(*S*)-4-((1-Methylheptyl)oxy)benzylidene-4′-(tetradecyloxy)aniline: mp 44.3 °C.

(*R*)-4-(Octyloxy)benzylidene-4′-((1-methylheptyl)oxy)aniline: mp 63.3 °C. ^{1}H-NMR (300 MHz, $CDCl_3$): δ 0.80–0.95 (m, 6H), 1.20–1.40 (m, 23H), 1.45 (m, 1H), 1.75 (m, 1H), 3.99 (t, J = 6.3 Hz, 2H), 4.32 (m, 1H), 6.87 (d, J = 8.6 Hz, 2H), 6.93 (d, J = 8.8 Hz, 2H), 7.15 (d, J = 8.6 Hz, 2H), 7.80 (d, J = 8.8 Hz, 2H), 8.38 (s, 1H). IR (neat) cm^{-1}: 1612 (ν C=N), 1247 (ν COC). Anal. Calcd for $C_{29}H_{43}NO_2$: C 79.59%, H 9.90%, N 3.20%. Found: C 79.85%, H 9.98%, N 3.15%.

Procedure To Obtain the Acetato-Bridged Palladium Dimers 8. To a suspension of 0.2 mmol of palladium acetate $Pd_3(OAc)_6$ in 20 mL of acetic acid was added the corresponding Schiff base (0.6 mmol), and the mixture was heated for ca. 15 h at 40 °C. With the exception of the precursor of complex **C**, all the compounds precipitated on cooling as

(27) Sierra, T.; Serrano, J. L.; Ros, M. B.; Ezcurra, A.; Zubía, J. *J. Am. Chem. Soc.* **1992**, *114*, 7645.

(28) Fukurawa, K.; Terashima, K.; Ichihashi, M.; Saitoh, S.; Miyazawa, K.; Inukai, T. *Ferroelectrics* **1988**, *85*, 451.

yellow solids contaminated with some palladium, which were filtered, washed with HOAc and EtOH, and dried. The complexes were then dissolved in dichloromethane, the traces of palladium were eliminated by filtration through a pad of Kieselguhr, and the pure complexes were isolated by evaporation of the solution to a small volume, addition of ethanol, and cooling. Yields: 77–89%.

The acetato-bridged dimer with four chiral chains was made from the chloro-bridged dimer C described below as follows: A mixture of C (100 mg) and NaOAc in a mixture of CH_2Cl_2/acetone (1/2, 30 mL) was refluxed for 2 h. The solution was evaporated to dryness, and the residue was extracted with 30 mL of CH_2Cl_2 and filtered through a pad of Kieselguhr to remove the sodium salts. Evaporation to dryness and trituration in cold EtOH afforded the desired complex in 73% yield.

Analytical Data for Complexes 8. Only two signals of the minor *cis* isomer are clearly seen in the ^{1}H-NMR spectra (300 MHz, $CDCl_3$) of all the complexes described below, which appear practically in the same position for all the complexes: δ 7.57 (s, 2H, two equivalent azomethine protons), 2.25 (s, 3H, one of the two inequivalent acetate methyls).[18] The composition of the mixtures and the chemical shifts of the two *trans* diastereoisomers are given below.

Acetato-bridged complex 8 precursor of complex (*S*)-A1: mixture (93.1/6.9) of *trans*/*cis* isomers, mp 159.5 °C. *Trans* isomer: mixture (69/31) of Λ-(*S*) and Δ-(*S*) diastereoisomers. Main diastereoisomer: ^{1}H-NMR (300 MHz, $CDCl_3$) δ 0.85–0.95 (m, 12H), 1.20–1.65 (m, 38H), 1.64–1.80 (m, 4H), 1.86 (s, 6H), 3.82–3.97 (m, 4H), 4.09–4.15 (m, 2H), 6.15 (d, J = 2.3 Hz, 2H), 6.53 (dd, J = 8.3 Hz, J = 2.3 Hz, 2H), 6.62, 6.68 (AB system, J = 9.0 Hz, 8H), 7.12 (d, J = 8.3 Hz, 2H), 7.47 (s, 2H). Minor diastereoisomer: 1.14 (d, J = 6.0 Hz, 6H), 1.80 (s, 6H), 4.19–4.30 (m, 2H), 6.18 (d, J = 2.2 Hz, 2H), 6.67, 6.77 (AB system, J = 8.8 Hz, 8H), 7.09 (d, J = 8.4 Hz,2H), 7.43 (s, 2H). IR (Nujol) cm^{-1}: 1610 (ν C=N), 1580, 1432 (ν C=O, overlapped bands), 1252 (ν COC). Anal. Calcd for $C_{58}H_{82}N_2O_8Pd_2$: C 60.68%, H 7.11%, N 2.44%. Found: C 61.12%, H 6.99%, N 2.42%.

Acetato-bridged complex 8 precursor of complex (*R*)-A1: mixture (93.0/7.0) of *trans*/*cis* isomers, mp 159.4 °C. *Trans* isomer: mixture (66/34) of Λ-(*R*) and Δ-(*R*) diastereoisomers. Main diastereoisomer: ^{1}H-NMR (300 MHz, $CDCl_3$) δ 0.85–0.95 (m, 12H), 1.20–1.65 (m, 38H), 1.64–1.76 (m, 4H), 1.85 (s, 6H), 3.82–3.96 (m, 4H), 4.06–4.15 (m, 2H), 6.11 (d, J = 2.3 Hz, 2H), 6.53 (dd, J = 8.3 Hz, J = 2.3 Hz, 2H), 6.62, 6.68 (AB system, J = 9.0 Hz, 8H), 7.11 (d, J = 8.3 Hz, 2H), 7.45 (s, 2H). Minor diastereoisomer: 1.12 (d, J = 6.0 Hz, 6H), 1.77 (s, 6H), 4.17–4.28 (m, 2H), 6.16 (d, J = 2.2 Hz, 2H), 6.67, 6.77 (AB system, J = 8.8 Hz, 8H), 7.09 (d, J = 8.4 Hz, 2H), 7.41 (s, 2H). IR (Nujol) cm^{-1}: 1610 (ν C=N), 1580, 1432 (ν C=O, overlapped bands), 1252 (ν COC). Anal. Calcd for $C_{58}H_{82}N_2O_8Pd_2$: C 60.68%, H 7.11%, N 2.44%. Found: C 60.80%, H 7.22%, N 2.42%.

Acetato-bridged complex 8 precursor of complex (*S*)-A2: mixture (93.5/6.5) of *trans*/*cis* isomers, mp 154.0 °C. *Trans* isomer: mixture (66/34) of Λ-(*S*) and Δ-(*S*) diastereoisomers. Main diastereoisomer: ^{1}H-NMR (300 MHz, $CDCl_3$) δ 0.80–0.92 (m, 12H), 1.20–1.54 (m, 46H), 1.64–1.76 (m, 4H), 1.85 (s, 6H), 3.76–4.00 (m, 4H), 4.00–4.15 (m, 2H), 6.10 (d, J = 1.9 Hz, 2H), 6.51 (dd, J = 8.3 Hz, J = 1.9 Hz, 2H), 6.61, 6.67 (AB system, J = 9.0 Hz, 8H), 7.11 (d, J = 8.3 Hz, 2H), 7.45 (s, 2H). Minor diastereoisomer: 1.13 (d, J = 5.8 Hz, 6H), 1.79 (s, 6H), 4.15–4.30 (m, 2H), 6.16 (d, J = 1.9 Hz, 2H), 6.66, 6.75 (AB system, J = 8.8 Hz, 8H), 7.07 (d, 2H) (masked with signal at 7.11), 7.41 (s, 2H). IR (Nujol) cm^{-1}: 1610 (ν C=N), 1582, 1430 (ν C=O, overlapped bands), 1252 (ν COC). Anal. Calcd for $C_{62}H_{90}N_2O_8Pd_2$: C 61.84%, H 7.53%, N 2.33%. Found: C 62.37%, H 7.43%, N 2.36%.

Acetato-Bridged Complex 8 precursor of complex (*R*)-A2: mixture (93.5/6.5) of *trans*/*cis* isomers, mp 155.0 °C. *Trans* isomer: mixture (67/33) of Λ-(*R*) and Δ-(*R*) diastereoisomers. Main diastereoisomer: ^{1}H-NMR (300 MHz, $CDCl_3$) δ 0.80–0.92 (m, 12H), 1.20–1.54 (m, 46H), 1.64–1.76 (m, 4H), 1.84 (s, 6H), 3.80–3.96 (m, 4H), 4.06–4.14 (m, 2H), 6.09 (d, J = 2.4 Hz, 2H), 6.52 (dd, J = 8.3 Hz, J = 2.4 Hz, 2H), 6.61, 6.67 (AB system, J = 9.0 Hz, 8H), 7.11 (d, J = 8.3 Hz, 2H), 7.45 (s, 2H). Minor diastereoisomer: 1.12 (d, J = 6.0 Hz, 6H), 1.78 (s, 6H), 4.17–4.26 (m, 2H), 6.16 (d, J = 2.2 Hz, 2H), 6.66, 6.75 (AB system, J = 8.8 Hz, 8H), 7.08 (d, J = 8.4 Hz, 2H), 7.41 (s, 2H). IR (Nujol) cm^{-1}: 1610 (ν C=N), 1583, 1430 (ν C=O, overlapped bands), 1254 (ν COC). Anal. Calcd for $C_{62}H_{90}N_2O_8Pd_2$: C 61.84%, H 7.53%, N 2.33%. Found: C 62.00%, H 7.43%, N 2.36%.

Acetato-bridged complex 8 precursor of complex (*S*)-A3: mixture (93.1/6.9) of *trans*/*cis* isomers, mp 143.5 °C. *Trans* isomer: mixture (69/31) of Λ-(*S*) and Δ-(*S*) diastereoisomers. Main diastereoisomer: ^{1}H-NMR (300 MHz, $CDCl_3$) δ 0.85–0.91 (m, 12H), 1.18–1.55 (m, 54H), 1.70–1.89 (m, 4H), 1.86 (s, 6H), 3.85–3.93 (m, 4H), 4.09–4.15 (m, 2H), 6.10 (d, J = 2.4 Hz, 2H), 6.53 (dd, J = 8.3 Hz, J = 2.4 Hz, 2H), 6.63, 6.68 (AB system, J = 9.0 Hz, 8H), 7.13 (d, J = 8.3 Hz, 2H), 7.47 (s, 2H). Minor diastereoisomer: 1.14 (d, J = 6.0 Hz, 6H), 1.80 (s, 6H), 4.18–4.24 (m, 2H), 6.18 (d, J = 2.3 Hz, 2H), 6.67, 6.77 (AB system, J = 8.8 Hz, 8H), 7.09 (d, 2H) (masked with signal at 7.13), 7.43 (s, 2H). IR (Nujol) cm^{-1}: 1610 (ν C=N), 1580, 1431 (ν C=O, overlapped bands), 1252 (ν COC). Anal. Calcd for $C_{66}H_{98}N_2O_8Pd_2$: C 62.89%, H 7.84%, N 2.22%. Found: C 63.20%, H 7.77%, N 2.15%.

Acetato-bridged complex 8 precursor of complex (*S*)-A4: mixture (93.7/6.3) of *trans*/*cis* isomers, mp 140.5 °C. *Trans* isomer: mixture (69/31) of Λ-(*S*) and Δ-(*S*) diastereoisomers. Main diastereoisomer: ^{1}H-NMR (300 MHz, $CDCl_3$) δ 0.82–0.91 (m, 12H), 1.20–1.54 (m, 70H), 1.68–1.82 (m, 4H), 1.84 (s, 6H), 3.85–3.97 (m, 4H), 4.06–4.16 (m, 2H), 6.0 (d, J = 2.2 Hz, 2H), 6.51 (dd, J = 8.1 Hz, J = 2.2 Hz, 2H), 6.60, 6.66 (AB system, J = 9.2 Hz, 8H), 7.11 (d, J = 8.1 Hz, 2H), 7.45 (s, 2H). Minor diastereoisomer: 1.12 (d, J = 6.2 Hz, 6H), 1.78 (s, 6H), 4.17–4.24 (m, 2H), 6.16 (d, J = 2.4 Hz, 2H), 6.67, 6.75 (AB system, J = 9.0 Hz, 8H), 7.07 (d, J = 8.4 Hz, 2H), 7.41 (s, 2H). IR (Nujol) cm^{-1}: 1609 (ν C=N), 1580, 1430 (ν C=O, overlapped bands), 1251 (ν COC). Anal. Calcd for $C_{74}H_{114}N_2O_8Pd_2$: C 64.76%, H 8.37%, N 2.04%. Found: C 64.89%, H 8.40%, N 2.12%.

Acetato-bridged complex 8 precursor of complex (*R*)-B2: mixture (91.6/8.4) of *trans*/*cis* isomers, mp 136.9 °C. *Trans* isomer: mixture (50/50) of the two *trans* diastereoisomers. One diastereoisomer: ^{1}H-NMR (300 MHz, $CDCl_3$) δ 0.80–0.90 (m, 12H), 1.20–1.60 (m, 46H), 1.64–1.80 (m, 4H), 1.82 (s, 6H), 3.58–3.72 (m, 2H), 3.72–3.85 (m, 2H), 4.22–4.34 (m, 2H), 6.09 (d, J = 2.2 Hz, 2H), 6.53 (dd, J = 2.2 Hz, J = 8.2 Hz, 2H), 6.58–6.72 (AB system overlapped with other signals, 8H), 7.07 (d, J = 8.2 Hz, 2H), 7.40 (s, 2H). The other diastereoisomer: 1.81 (s, 6H), 3.58–3.72 (m, 2H), 3.72–3.85 (m, 2H), 4.22–4.34 (m, 2H), 6.10 (d, J = 2.2 Hz, 2H), 6.54 (dd, J = 2.2 Hz, J = 8.2 Hz, 2H), 6.58–6.72 (AB system overlapped with other signals, 8H), 7.08 (d, J = 8.2 Hz, 2H), 7.41 (s, 2H). IR (Nujol) cm^{-1}: 1612 (ν C=N), 1576, 1415 (ν C=O, overlapped bands), 1252 (ν COC). Anal. Calcd for $C_{62}H_{90}N_2O_8Pd_2$: C 61.84%, H 7.53%, N 2.33%. Found: C 62.26%, H 7.63%, N 2.29%.

Acetato-bridged complex 8 with four chiral chains: mixture (93.2/6.8) of *trans*/*cis* isomers, mp 110.5 °C. *Trans* isomer: mixture (64/36) of the two *trans* diastereoisomers. Main diastereoisomer: ^{1}H-NMR (300 MHz, $CDCl_3$) δ 0.80–0.92 (m, 12H), 1.20–1.54 (m, 42H), 1.65–1.80 (m, 8H) 1.82 (s, 6H), 4.30–4.45 (m, 4H), 6.18 (d, J = 2.3 Hz, 2H), 6.54 (dd, J = 8.3 Hz, J = 2.3 Hz, 2H), 6.65, 6.72 (AB system, J = 8.9 Hz, 8H), 7.11 (d, J = 8.3 Hz, 2H), 7.45 (s, 2H). Minor diastereoisomer: 1.19 (d, J = 6.1 Hz, 6H), 1.72 (s, 6H), 4.10–4.25 (m, 4H), 6.24 (d, J = 2.1 Hz, 2H), 6.50–6.55 (dd, 2H, overlapped signals), 6.70 (d, 4H, overlapped signals), 6.81 (d, J = 8.9 Hz, 4H), 7.08 (d, J = 8.3 Hz, 2H), 7.41 (s, 2H). IR (Nujol) cm^{-1}: 1608 (ν C=N), 1575, 1420 (ν C=O), 1254 (ν COC). Anal. Calcd for $C_{62}H_{90}N_2O_8Pd_2$: C 61.84%, H 7.53%, N 2.44%. Found: C 61.62%, H 7.17%, N 2.33%.

Procedure To Obtain the Chloro-Bridged Palladium Complexes 9. To a stirred solution of the corresponding acetato-bridged complex (0.2 mmol) in 30 mL of dichloromethane was added the stoichiometric amount of a methanolic solution of hydrogen chloride (HCl/OAc = 1/1). After stirring at room temperature for 1 h the solution was evaporated to dryness. Addition of acetone/ethanol afforded the chloro-bridged complexes as yellow solids, which were purified by chromatography on a silica gel column; CH_2Cl_2 was used as eluant. Yields: 50–85%.

For complex C the procedure was as follows: To a suspension of 300 mg (0.45 mmol) of palladium acetate $Pd_3(OAc)_6$ in 20 mL of acetic acid was added the corresponding Schiff base (600 mg, 1.37 mmol), and the mixture was heated for ca. 15 h at 40 °C. The solution was evaporated to dryness in vacuum. The residue was dissolved in dichloromethane (30 mL), and HCl was added (1.33 mmol, 3.5 mL of a 0.358 N solution in MeOH). After stirring for 1 h the solution was evaporated to dryness in vacuum. The residue was chromatographed, using dichloromethane as eluant, in a 20-cm silica gel column where the traces of palladium and acetato-bridged complexes are retained. The eluted solution was evaporated to dryness and the residue triturated in cold ethanol to give complex C in 71% yield.

Analytical Data for Complexes 9. Complex (*S*)-A1: ^{1}H-NMR (300 MHz, $CDCl_3$) δ 0.83–0.92 (m, 12H), 1.20–1.60 (m, 38H), 1.60–1.95 (m, 4H), 3.94 (t, J = 6.2 Hz, 4H), 4.26–4.46 (m, 2H), 6.51 (d, J = 8.2 Hz, 2H), 6.78 (overlapped signals, 2H), 6.85 (d, J = 8.4 Hz, 4H), 7.16 (d, J = 8.2 Hz, 2H), 7.26 (d, 4H, overlapped with $CHCl_3$ signal), 7.75 (s, 2H). IR (Nujol) cm^{-1}: 1609 (ν C=N), 1251 (ν COC), 266, 259 (ν

PdCl). Anal. Calcd for $C_{54}H_{76}N_2O_4Cl_2Pd_2$: C 58.91%, H 6.96%, N 2.54%. Found: C 59.09%, H 7.09%, N 2.66%.

Complex (*R*)-A1: spectroscopic data identical to those of (*S*)-**A1**. Anal. Calcd for $C_{54}H_{76}N_2O_4Cl_2Pd_2$: C 58.91%, H 6.96%, N 2.54%. Found: C 59.21%, H 6.40%, N 2.61%.

Complex (*S*)-A2: ^{1}H-NMR (300 MHz, $CDCl_3$) δ 0.82–0.92 (m, 12H), 1.20–1.50 (m, 46H), 1.62–1.84 (m, 4H), 3.94 (t, J = 6.0 Hz, 4H), 4.28–4.50 (m, 2H), 6.51 (d, J = 8.2 Hz, 2H), 6.79 (overlapped signals, 2H), 6.84 (d, J = 8.2 Hz, 4H), 7.16 (d, J = 8.2 Hz, 2H), 7.26 (d, 4H, overlapped with $CHCl_3$ signal), 7.75 (s, 2H). IR (Nujol) cm^{-1}: 1612 (ν C=N), 1260 (ν COC), 266, 259 (ν PdCl). Anal. Calcd for $C_{58}H_{84}N_2O_4Cl_2Pd_2$: C 60.21%, H 7.32%, N 2.42%. Found: C 60.78%, H 7.38%, N 2.54%.

Complex (*R*)-A2: spectroscopic data identical to those of (*S*)-**A2**. Anal. Calcd for $C_{58}H_{84}N_2O_4Cl_2Pd_2$: C 60.21%, H 7.32%, N 2.42%. Found: C 60.29%, H 7.27%, N 2.46%.

Complex (*S*)-A3: ^{1}H-NMR (300 MHz, $CDCl_3$) δ 0.82–0.95 (m, 12H), 1.20–1.60 (m, 54H), 1.60–1.80 (m, 4H), 3.94 (t, J = 6.0 Hz, 4H), 4.28–4.50 (m, 2H), 6.51 (d, J = 8.2 Hz, 2H), 6.78 (overlapped signals, 2H), 6.84 (d, J = 8.4 Hz, 4H), 7.16 (d, J = 8.2 Hz, 2H), 7.26 (d, 4H, overlapped with $CHCl_3$ signal), 7.76 (s, 2H). IR (Nujol) cm^{-1}: 1607 (ν C=N), 1253 (ν COC), 250, 264 (ν PdCl). Anal. Calcd for $C_{62}H_{92}N_2O_4Cl_2Pd_2$: C 61.39%, H 7.64%, N 2.31%. Found: C 61.56%, H 8.10%, N 2.34%.

Complex (*S*)-A4: ^{1}H-NMR (300 MHz, $CDCl_3$) δ 0.82–0.92 (m, 12H), 1.20–1.60 (m, 70H), 1.70–1.84 (m, 4H), 3.94 (t, J = 5.9 Hz, 4H), 4.28–4.50 (m, 2H), 6.51 (d, J = 8.2 Hz, 2H), 6.78 (overlapped signals, 2H), 6.84 (d, J = 8.4 Hz, 4H), 7.16 (d, J = 8.2 Hz, 2H), 7.26 (d, 4H, overlapped with $CHCl_3$ signal), 7.75 (s, 2H). IR (Nujol) cm^{-1}: 1606 (ν C=N), 1254 (ν COC), 250, 267 (ν PdCl). Anal. Calcd for $C_{70}H_{108}N_2O_4Cl_2Pd_2$: C 63.44%, H 8.21%, N 2.11%. Found: C 63.23%, H 8.20%, N 2.04%.

Complex (*R*)-B2: ^{1}H-NMR (300 MHz, $CDCl_3$) δ 0.80–0.95 (m, 12H), 1.20–1.50 (m, 46H), 1.62–1.84 (m, 4H), 3.96 (t, J = 6.0 Hz, 4H), 4.31–4.41 (m, 2H), 6.52 (d, J = 8.2 Hz, 2H), 6.80 (overlapped signals, 2H), 6.83 (d, J = 8.4 Hz, 4H), 7.17 (d, J = 8.2 Hz, 2H), 7.26 (d, 4H, overlapped with $CHCl_3$ signal), 7.76 (s, 2H). IR (Nujol) cm^{-1}: 1610 (ν C=N), 1251 (ν COC), 257, 252 (ν PdCl). Anal. Calcd for $C_{58}H_{84}N_2O_4Cl_2Pd_2$: C 60.21%, H 7.32%, N 2.42%. Found: C 60.38%, H 7.38%, N 2.38%.

Complex (*R*)-C: ^{1}H-NMR (300 MHz, $CDCl_3$) δ 0.82–0.98 (m, 12H), 1.18–1.50 (m, 44H), 1.62–1.80 (m, 8H), 4.20–4.60 (m, 4H), 6.51 (d, J = 8.2 Hz, 2H), 6.80 (overlapped signal, 2H), 6.83 (d, J = 8.2 Hz, 4H), 7.16 (d, J = 8.2 Hz, 2H), 7.28 (d, 4H, overlapped with $CDCl_3$ signal), 7.76 (s, 2H). IR (Nujol) cm^{-1}: 1610 (ν C=N), 1250 (ν COC), 258, 244 (ν PdCl). Anal. Calcd for $C_{58}H_{84}N_2O_4Cl_2Pd_2$: C 60.21%, H 7.32%, N 2.42%. Found: C 60.26%, H 7.35%, N 2.34%.

Techniques. Microanalysis was performed with a Perkin-Elmer 240-B microanalyzer. Infrared spectra for all the compounds were obtained by using a Perkin-Elmer 883 spectrometer in the 200–4000-cm^{-1} spectral range. ^{1}H NMR spectra were recorded on a Varian Unity 300 spectrometer operating at 300 MHz for ^{1}H. The polarimetry measurements were carried out with a Perkin-Elmer 241-C polarimeter.

The textures of the mesophases were studied with a Nikon optical microscope equipped with a polarizing light, a Mettler FP82 hot stage, and a Mettler FP80 central processor. Measurements of temperatures of transition were carried out using a Perkin-Elmer DSC-7 differential scanning calorimeter with a heating and cooling rate of 10 °C min^{-1} (the apparatus was calibrated with indium, 156.6 °C, and tin, 232.1 °C).

Powder X-ray diffraction patterns were obtained in a Guinier diffractometer (Huber 644) operating with a Cu Kα_1 beam issued from a germanium monochromator. The samples were held in rotating Lindemann glass capillaries (ϕ = 0.5 mm) and heated with a variable-temperature attachment. The diffraction patterns were registered with a scintillation counter.

The spontaneous polarization and the response time were obtained simultaneously using the triangular wave form method,[29,30] using fields of 10–50 Hz and 1 Hz (complex **C**) and voltages peak to peak of 400–1000 V. In the experimental setup the triangular wave voltage is supplied by a HP3325A function generator and then magnified by a KEPCO amplifier. The current–voltage cycles are recorded by a digital acquisition system HP7090A. All the experiment is interfaced to a microcomputer. Cells for these measurements were made of two gold-brass electrodes of 12-μm diameter and 100-μm thickness, covered with a thin film of polyvinyl alcohol, and rubbed in one direction.

The Ps signs were determined by the field reversal method through optical observation of the extinction direction by rotating the stage according to Lagerwall's convention.[1a] For these measurements 10-μm cells with indium tin oxide (ITO) electrodes coated with polyimides were used.

The binary mixtures of the chiral ligands with the achiral host (4-(hexyloxy)phenyl 4′-(decycloxy)benzoate; K 62.5 °C SmC 78.2 °C SmA 84.5 °C N 90.5 °C I) were prepared by weighing the appropriate amounts of each component and mixing with stirring in the isotropic phase for 1 min. The mixture was then allowed to cool. This operation was repeated twice.

Acknowledgment. This work was financed by the Comisión Interministerial de Ciencia y Tecnologia (Spain, Projects MAT90-0325, MAT90-0813, and MAT91-0962CO2-01) and the Consejeria de Cultura de la Junta de Castilla y León (Spain). M.J.B. thanks IBERDUERO for a studenship.

(29) Miyasato, K.; Abe, S.; Takezoe, H.; Fukuda, A.; Kuze, E. *Jpn. J. Appl. Phys.* **1983**, *22*, L661.

(30) De la Fuente, M. R.; Ezcurra, A.; Pérez-Jubindo, M. A.; Zubía, J. *Liq. Cryst.* **1990**, *7*, 51.